

Architecture-Agnostic Feature Synergy for Universal Defense Against Heterogeneous Generative Threats

Bingxue Zhang
zhangbingxue@usst.edu.cn
University of Shanghai for Science
and Technology
Shanghai, China

Yang Gao
gaoyang@st.usst.edu.cn
University of Shanghai for Science
and Technology
Shanghai, China

Feida Zhu
fdzhu@smu.edu.sg
Singapore Management University
Singapore, Singapore

Yanyan Shen
shenyy@sjtu.edu.cn
Shanghai Jiao Tong University
Shanghai, China

Yang Shi
shiyang1121@st.usst.edu.cn
University of Shanghai for Science
and Technology
Shanghai, China

Abstract

The ubiquitous deployment of Generative AI has precipitated unprecedented challenges in content safety and privacy. However, prevailing defense mechanisms are often tailored to specific model architectures (e.g., solely targeting Diffusion Models or GANs), resulting in fragile “defense silos” that exhibit poor generalization against heterogeneous and often agnostic generative threats in the wild. This paper diagnoses a fundamental optimization barrier in naive pixel-space ensemble strategies: owing to inherently divergent objective functions, pixel-level gradients from heterogeneous generators become statistically orthogonal, causing destructive interference during joint optimization. To break this bottleneck, we propose an observation based on empirical evidence: despite disparate pixel-space optimization landscapes, the high-level feature representations of generated content exhibit alignment across different architectures. Grounded in this observation, we devise an Architecture-Agnostic Targeted Feature Synergy (ATFS) framework. By introducing a target guidance image, ATFS reformulates multi-model defense as a unified feature space alignment task, thereby enabling intrinsic gradient alignment at the feature level without complex rectification. Extensive experiments show that ATFS achieves SOTA protection in heterogeneous scenarios (e.g., Diffusion+GAN). It converges rapidly, reaching >90% performance within 40 iterations, and retains strong attack potency even under a tight perturbation budget ($\epsilon=2/255$). The framework seamlessly extends to unseen architectures (e.g., VQ-VAE) by simply switching the feature extractor, and demonstrates superior robustness against interference such as JPEG compression and scaling. Being computationally efficient and lightweight, ATFS offers a viable pathway to dismantle defense silos and pave the way for a universal generative security framework. Code and models are open-sourced to ensure reproducibility and facilitate adoption.

Keywords

Generative AI Security, Proactive Defense, Model-Agnostic Defense, Cross-Modal Feature Isomorphism, Feature Synergy

1 Introduction

The explosive growth of Generative Artificial Intelligence has fundamentally transformed content creation and digital media editing. Technologies ranging from text-to-image diffusion models [1] to GAN-based deepfakes [2] provide creators with unprecedented realism and accessibility. However, this democratization of creativity simultaneously introduces severe risks to content security, privacy, and societal trust [3]. Malicious actors can readily exploit these tools to create unauthorized portrait manipulations [4], fabricate digital evidence, and generate large-scale disinformation, posing systemic risks to the integrity of our information ecosystem [5]. In this work, we focus on defending facial images against unauthorized editing and forgery by heterogeneous generative models.

In response, proactive defense mechanisms have been developed to preemptively protect visual content [6, 7]. The core principle involves embedding imperceptible perturbations into original images to disrupt the generation process of malicious models. Despite considerable progress, a critical limitation persists in current defense paradigms: architecture specificity. Existing methods are typically optimized for a single family of generative models [8]. For example, defenses targeting diffusion models often perturb denoising trajectories [9], while those designed for GANs attack discriminative boundaries [10]. This targeted optimization creates isolated “defense silos,” where a method effective against one architecture fails completely against another.

The real-world threat landscape, however, is heterogeneous and agnostic. A defender cannot anticipate whether an attacker will employ a diffusion model, a GAN, or an entirely unseen system. As visually demonstrated in Figure 1, perturbations crafted for a diffusion model [1] become ineffective against a GAN [11], and vice versa. This defense silo phenomenon critically undermines the practical reliability of existing techniques in open environments [12], especially in protecting sensitive visual content such as human portraits.

A naive strategy to bridge these silos is to simply combine attacks against multiple models. This paper first reveals the fundamental reason this intuitive approach fails. Heterogeneous generative models are driven by distinct optimization objectives: Diffusion models guide gradients via score matching for density estimation

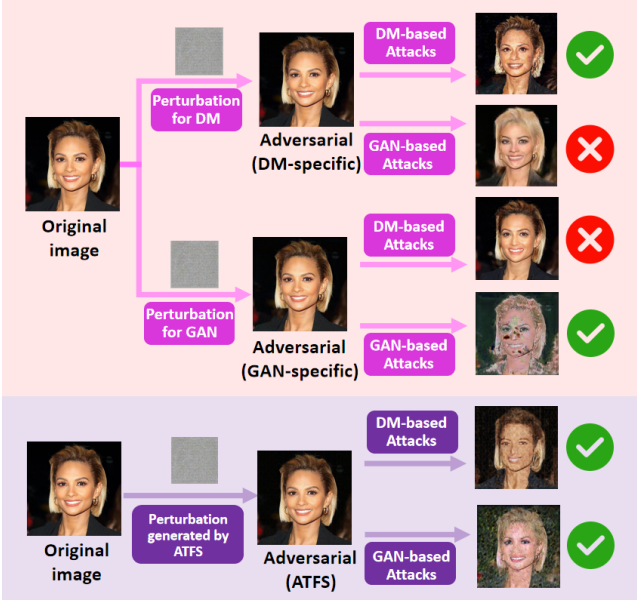


Figure 1: Defense Silos Phenomenon: Architecture-Specific Attacks Fail Cross-Model. The figure illustrates how perturbations optimized for one model architecture fail to transfer to another. A checkmark (✓) indicates successful defense (editing failure), while a cross (×) indicates defense failure (editing success). Facial images protected by diffusion-specific methods remain vulnerable to GAN-based edits, and vice versa.

[13], whereas GANs direct gradients toward adversarial discriminative boundaries [2]. We demonstrate that this intrinsic objective divergence causes their gradient vectors in pixel space to be statistically orthogonal in high dimensions [14]. Consequently, joint optimization leads to destructive interference rather than synergy. While gradient mitigation algorithms like PCGrad [15] exist, they incur significant computational costs and fail to resolve the deeper geometric incompatibility between these paradigms [16].

To transcend this optimization barrier, we propose a paradigm shift: moving from pixel-level conflict to feature-level consensus. We introduce an observation based on empirical evidence: despite disparate low-level generation mechanisms, all models capable of producing perceptually plausible content map inputs onto high-level feature spaces that exhibit alignment for similar perceptual content. This observed alignment in feature spaces provides the practical foundation for a unified, model-agnostic defense.

Guided by this insight, we propose the Architecture-Agnostic Targeted Feature Synergy (ATFS) framework. ATFS leverages a shared target feature direction—derived from a guide image—to transform the multi-model defense problem into a unified feature space alignment task. Theoretical analysis shows that under this formulation, the originally conflicting pixel-level gradients become directionally aligned when projected through the feature extractors, inducing constructive interference. This alignment enables efficient collaborative defense without the need for computationally expensive gradient surgery [17].

The main contributions of this paper are summarized as follows:

1) We provide an analysis demonstrating that gradient conflicts among heterogeneous generative models in pixel space are fundamental, limiting the effectiveness of existing ensemble methods. Based on empirical observations of feature space alignment across different architectures, we propose a new perspective for constructing model-agnostic defense frameworks.

2) Guided by this perspective, we design the ATFS framework. By aligning models in a shared feature space via a target feature direction, it unifies multi-model defense into a single optimization task, achieving gradient synergy without complex gradient manipulation. The framework is lightweight and scalable; extending protection to a new model requires only integrating its feature extractor.

3) We conduct comprehensive evaluations on facial image protection across multiple heterogeneous threat scenarios. Experiments demonstrate that ATFS significantly outperforms all baseline methods in defense effectiveness and exhibits strong robustness against signal disruptions. Crucially, we incorporate a fairness-by-design analysis into defense research, proving that its protective effects remain consistent across different demographic attributes, avoiding algorithmic bias.

4) To foster the development of the trustworthy AI community, we have fully open-sourced our code and models. This not only ensures research reproducibility but also provides an auditable defense tool for subsequent researchers, contributing to the standardized assessment of generative model safety.

2 Related Work

This section provides a systematic review of the proactive defense landscape for Generative AI and related techniques. We first review defense methods tailored to specific generative architectures, then analyze research on adversarial transferability and ensemble strategies, and finally discuss classical approaches for resolving gradient conflicts in multi-objective optimization.

2.1 Architecture-Specific Proactive Defense

With the proliferation of deep generative models, Proactive Defense has emerged as a frontier technique for safeguarding image copyright and privacy [18]. Existing methods can be broadly categorized into two streams based on their target model architectures:

Defenses against Diffusion Models: These works primarily aim to disrupt the denoising generation process of diffusion models (e.g., Stable Diffusion [1]). Glaze [18] pioneered the concept of Style Cloaking, minimizing the distance to a target style in feature space to mislead the model’s learning of artist styles. Mist [9] further exploited the model’s reliance on texture and content, generating adversarial examples that possess both high transferability and imperceptibility. PhotoGuard [18] focuses on defending against image editing (e.g., Inpainting) by attacking the latent space encoding process to induce generation errors.

Defenses against Generative Adversarial Networks (GANs): This line of research aims to sabotage the editing and forgery capabilities of GANs (e.g., models used for face swapping [4]). Anti-Forgery [10] proposed a perception-based perturbation attack designed to disrupt GANs’ image editing abilities. CMUA-Watermark [19] attempted to add cross-model universal watermarks to facial images to defend

against attacks from multiple Face-Swapping models. Additionally, FakeTagger[3] achieved passive tracking of GAN-generated content by embedding recoverable adversarial information into images.

Despite their success against specific targets, these methods suffer from severe Architecture-Specificity. Perturbations designed for diffusion models (e.g., Mist[9]) struggle to transfer to GANs[10], and vice versa. This phenomenon of "defense silos" renders existing technologies ill-equipped to handle complex, real-world threat environments where model types are unknown or multiple architectures coexist[6].

2.2 Adversarial Transferability and Ensemble Strategies

In discriminative tasks such as image classification, the transferability of adversarial examples is a core research question[7]. Since high-performing classifiers (e.g., ResNet and ViT) tend to learn similar decision boundaries, the adversarial gradient directions generated against them are often highly consistent. Classical ensemble attack strategies[7] leverage this gradient alignment property, significantly enhancing cross-model transferability by simply aggregating losses or gradients from multiple models.

However, directly transferring this ensemble strategy to the defense of generative models faces fundamental challenges. The core objective of generative models (e.g., Diffusion Models, GANs) is to construct complex data distributions rather than perform simple classification. Research indicates that models with different generative paradigms possess essentially different optimization objectives and loss functions[8]. For instance, diffusion models learn the gradient field of the data distribution via score matching, while GANs optimize a generator and discriminator through a minimax game[2]. This fundamental disparity in objective functions renders their geometric relationships in pixel-level gradients incompatible[16]. Consequently, the efficacy of directly applying ensemble strategies successful in discriminative tasks to generative defense remains unclear, and such approaches face the risk of optimization conflicts. How to achieve effective joint attacks against heterogeneous generative models remains an open problem.

2.3 Multi-Objective Optimization and Gradient Conflict

From an optimization perspective, defending against multiple heterogeneous models simultaneously is a quintessential multi-objective optimization problem, where loss functions for different models may produce conflicting gradients. The field of Multi-Task Learning (MTL) has proposed various algorithms to resolve such gradient conflicts. PCGrad[15] is the most widely used conflict-removal algorithm, which eliminates negative interference by projecting the gradient of a conflicting task onto the normal plane of the other. GradNorm[20] addresses gradient magnitude imbalance by dynamically adjusting loss weights for each task. MGDA[16] seeks a Pareto-optimal common descent direction by solving a quadratic programming problem.

While these methods have proven effective in training multi-task neural networks with shared parameters, directly applying them to the specific scenario of proactive defense for generative models has limitations. First, adversarial attacks typically require dozens

of iterations; the additional computational overhead introduced by algorithms like PCGrad and MGDA (e.g., projections, solving QP problems) may compromise real-time performance. More importantly, these methods generally assume a latent compatibility between tasks in the parameter space. In contrast, the gradient conflicts of heterogeneous generative models in pixel space likely stem from the deep geometric incompatibility of their optimization landscapes[15]. Therefore, forcing Gradient Surgery in pixel space struggles to fundamentally resolve conflicts and may lead optimization toward inefficient compromise solutions.

3 Method

3.1 Motivation and Problem Formulation

The rapid advancement of generative AI has led to the emergence of distinct "defense silos" in architecture-specific protection methods, as discussed in the introduction. These methods often fail to provide universal protection against heterogeneous generative models due to fundamental divergence in their optimization objectives. This section aims to formalize the cross-model defense problem, identify its underlying challenges, and establish the theoretical foundation for our approach.

3.1.1 Formalization of the Heterogeneous Defense Problem. Given K heterogeneous generative models $\{M_k\}_{k=1}^K$ (e.g., diffusion models, generative adversarial networks, etc.), each with its own distinct generation mechanism. Let $L_k(x)$ denote the attack loss function targeting model M_k , whose goal is to disrupt the normal generation or editing capability of that model. A general cross-model defense method aims to find a minimal perturbation δ that is simultaneously effective against all models:

$$\max_{\|\delta\|_\infty \leq \epsilon} \sum_{k=1}^K \omega_k L_k(x + \delta) \quad (1)$$

where ω_k represents the weight assigned to each model, ϵ is the perturbation budget, and $\|\delta\|_\infty < \epsilon$ ensures the perturbation remains visually imperceptible.

3.1.2 Analysis of Gradient Conflict in Pixel Space. Although directly optimizing Equation (1) appears straightforward, we observe that this approach faces fundamental challenges in practice. The optimization objectives of different generative models are inherently distinct: diffusion models learn the gradient field of the data distribution via score matching, while GANs optimize the generator and discriminator through a minimax game. This divergence in objectives leads their gradient directions in pixel space to become nearly orthogonal:

$$\mathbb{E}[\langle \nabla_x L_D, \nabla_x L_G \rangle] \approx 0 \quad (2)$$

where L_D and L_G denote the attack losses for diffusion models and GANs, respectively. This gradient orthogonality causes destructive interference during joint optimization, often resulting in stagnation or oscillation of the optimization process and preventing the accumulation of effective perturbations.

3.1.3 Heuristic Observation: Feature Space Alignment. To overcome the optimization bottleneck in pixel space, we propose a key empirical observation: despite differences in their low-level mechanisms,

all generative models must capture high-level feature information from input images to produce plausible content. This observation is grounded in a widely accepted design principle: the encoder layers of modern generative models are intentionally designed to extract image features that drive subsequent generation.

Specifically, for any generative model M_k capable of producing human-perceptible content, we can identify a feature extraction function $\Phi_k : \mathcal{X} \rightarrow \mathcal{F}_k$ that maps the input image into a low-dimensional feature space \mathcal{F}_k . We observe that for visually similar content, the feature representations extracted by different models exhibit a degree of alignment. This observation suggests a new defense paradigm: rather than reconciling conflicting optimization directions in pixel space, we can seek consensus in higher-level feature spaces.

3.2 Shared Feature Space Alignment Framework

Building on the observations above, we propose the Architecture-agnostic Targeted Feature Synergy (ATFS) framework. The core idea of ATFS is to avoid direct optimization in the conflicting pixel space. Instead, it unifies the defense problem against heterogeneous models into a coordinated optimization task within a high-level feature space, guided by a shared target feature direction.

3.2.1 Feature Extraction and Shared Feature Space. We first define an accessible feature extraction function $\Phi_k : \mathcal{X} \rightarrow \mathcal{F}_k$ for each generative model M_k to be defended. This function maps the input image x to a model-specific, low-dimensional feature space \mathcal{F} . The choice of this function corresponds to the layer within the model responsible for encoding high-level information:

1) For Diffusion Models (e.g., Stable Diffusion): We select the output features of its VAE encoder. This layer compresses the distributional information of the image and is highly sensitive to both content and style.

2) For Generative Adversarial Networks (e.g., StarGAN): We select the deep activation maps from the generator’s encoder. These features directly determine the high-level attributes and structure of the generated image.

3) For Other Architectures (e.g., VQ-VAE): We select the feature representation from the encoder’s output.

This selection is based on a straightforward engineering fact: to generate plausible content, a generative model must form a high-level understanding of the input somewhere in its architecture. Therefore, although their numerical forms differ, the function Φ_k serves as a proxy representation for how each model "understands" the input image. Our empirical observation indicates that for the same perceptual content, the features $\Phi_k(x)$ from different models tend to encode similar concepts within their respective spaces. This suggests they inhabit an empirically shared abstract feature space.

3.2.2 Feature Space Synergistic Optimization Mechanism. To achieve synergy within this shared feature space, we introduce a target guidance image x_{tgt} . This image does not need to share any feature correlation with the original image x ; its purpose is to provide a clear and consistent target for feature change.

For each model M_k , we pre-compute its feature representation of this target image, termed the target feature vector:

$$t_k = \Phi_k(x_{tgt}) \quad (3)$$

All t_k remain fixed during optimization, forming a global alignment target set.

Our defense objective thus shifts: we seek a minimal perturbation δ such that the representation of the perturbed image $x + \delta$ in each model’s feature space simultaneously deviates from its original position and moves towards its respective target feature vector t_k . This defines a unified objective function:

$$\min_{\|\delta\|_\infty \leq \epsilon} J(\delta) = \sum_{k=1}^K \omega_k \cdot \underbrace{\|\Phi_k(x + \delta) - t_k\|_2^2}_{L_k^{\text{align}}(x+\delta)} \quad (4)$$

where ω_k are the model weights (typically set equally), and ϵ is the perturbation budget. Optimizing this objective function essentially forces all models to develop a consistent, feature-level misinterpretation of the perturbed image, aligning it towards x_{tgt} .

3.2.3 Working Mechanism of Feature Synergy. The ability of this method to circumvent gradient conflicts in pixel space stems from its inherent synergy within the feature space. The gradient of the loss function L_k^{align} with respect to the input is:

$$\nabla_x L_k^{\text{align}} = 2 \cdot \mathbf{J}_{\Phi_k}^\top(x) \cdot (\Phi_k(x) - t_k) \quad (5)$$

where $\mathbf{J}_{\Phi_k}(x)$ is the Jacobian matrix of the feature extraction function in x .

Two key factors contribute to gradient alignment: 1) The optimization goal for all models is to reduce the distance to their fixed target t_k . Due to the empirical alignment of the feature spaces in the models, the difference vector $\Phi_k(x) - t_k$ implies a similar direction of high-level feature change. 2) $\mathbf{J}_{\Phi_k}(x)$ restores the changes from the feature space to the pixel space. Since Φ_k is designed to be sensitive to high-level feature changes, the principal directions of its Jacobian correspond to structural changes in the image most relevant to feature expression.

Consequently, although the Jacobians \mathbf{J}_{Φ_k} differ mathematically across models, they all map a similar "intent of feature distortion" into pixel space. This causes the final pixel-space gradients $\nabla_x L_k^{\text{align}}$ to align in direction, resulting in constructive superposition rather than mutual cancellation. This mechanism allows us to efficiently generate adversarial perturbations effective against multiple heterogeneous models simultaneously, without requiring complex gradient surgery.

3.3 Algorithm Implementation and Details

This section details the concrete implementation steps, optimization procedure, and key design choices of the ATFS framework to ensure reproducibility.

3.3.1 Optimization Algorithm. Algorithm 1 outlines the complete workflow of ATFS. Its core objective is to iteratively minimize the feature alignment loss defined in Section 3.2.2, thereby generating adversarial perturbations effective against multiple heterogeneous models simultaneously. A flowchart is shown in Figure 2.

The algorithm consists of two phases. The first phase (lines 2-5) involves precomputing target features. Here, the fixed target feature

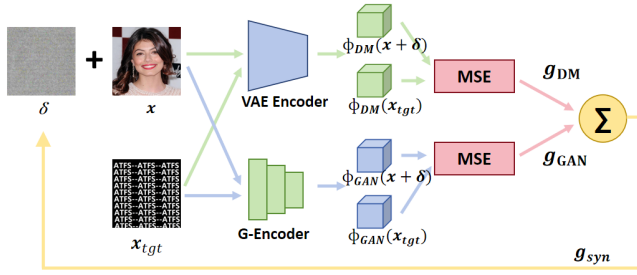


Figure 2: Universal Feature Anchoring: Unifying Heterogeneous Models via Shared Feature Space

Algorithm 1 Architecture-Agnostic Targeted Feature Synergy (ATFS)

Require: Target Models $\{M_k\}_{k=1}^K$; Clean Image x ; Target Image x_{tgt} ; Feature Extractors $\{\Phi_k\}_{k=1}^K$; Budget ϵ , Steps T , Step size α .

Ensure: Adversarial Example x_{adv} .

```

1: Initialize:  $x^{(0)} \leftarrow x, \delta_0 \leftarrow 0$ 
2:
3:   Phase 1: Precompute Target Features
4:   for  $k = 1$  to  $K$  do
5:      $t_k \leftarrow \Phi_k(x_{tgt})$   $\triangleright$  Extract target feature direction
6:   end for
7:   Phase 2: Synergistic Optimization Loop
8:   for  $t = 0$  to  $T - 1$  do
9:      $g_{syn} \leftarrow 0$   $\triangleright$  Initialize synergistic gradient
10:    for  $k = 1$  to  $K$  do
11:       $f_k \leftarrow \Phi_k(x + \delta_t)$   $\triangleright$  Forward pass
12:       $\mathcal{L}_k \leftarrow \|f_k - t_k\|_2^2$   $\triangleright$  Feature Alignment Loss
13:       $g_k \leftarrow \nabla_{\delta} \mathcal{L}_k$   $\triangleright$  Compute gradient
14:       $\hat{g}_k \leftarrow g_k / (\|g_k\|_2 + \xi)$   $\triangleright$  Gradient normalization
15:       $g_{syn} \leftarrow g_{syn} + \omega_k \cdot \hat{g}_k$   $\triangleright$  Accumulate gradients
16:    end for
17:     $\delta_{t+1} \leftarrow \text{Clip}_{[-\epsilon, \epsilon]}(\delta_t - \alpha \cdot \text{sign}(g_{syn}))$   $\triangleright$  Update Perturbation via PGD
18:  end for
19:   $x_{adv} \leftarrow \text{Clip}_{[0, 1]}(x + \delta_T)$ 
20:  return  $x_{adv}$ 

```

vectors t_k are extracted from the target image x_{tgt} for each model, serving as a common guide for optimization. The second phase (lines 7-19) is the synergistic optimization loop. Its goal is to find a perturbation δ such that the features f_k of the perturbed image simultaneously move closer to their respective targets t_k . In each iteration, the algorithm computes the loss gradient for each model, normalizes it, and then aggregates these gradients linearly into a synergistic gradient g_{syn} . Finally, the perturbation is updated using Projected Gradient Descent (PGD).

3.3.2 Key Implementation Details. *Target Image Selection:* As indicated in the algorithm input, x_{tgt} can be any image unrelated to the original x . To maximize distortion in the feature space, we select target images with strong, structured visual patterns that provide a clear and significantly divergent direction from the original features. Specifically, drawing from classical research in image

perception and adversarial pattern design, we employ three types of patterns widely recognized for eliciting strong visual responses: (1) high-contrast stripes, (2) Moiré patterns, and (3) overly busy textures. The feature distributions of these patterns differ markedly from natural images, effectively guiding the optimization process toward substantial and consistent shifts in the feature space.

Gradient Normalization: This step is crucial for achieving effective synergy. Significant differences in feature dimensions, activation magnitudes, and loss surface scales across models can cause the optimization to be dominated by the model with the largest gradient magnitude if raw gradients g_k are summed directly. We apply L_2 normalization to each model's gradient:

$$\hat{g}_k = \frac{g_k}{\|g_k\|_2 + \xi} \quad (6)$$

where ξ is a small constant (e.g., 10^{-8}) for numerical stability. This ensures that during gradient aggregation, each model's contribution is determined by its gradient direction rather than its magnitude, leading to a fair and effective fusion of optimization signals from heterogeneous models.

4 Experiments

This section empirically evaluates the proposed Architecture-Agnostic Targeted Feature Synergy (ATFS) framework. We design a series of qualitative and quantitative experiments to address five core Research Questions (RQs), validating the method's effectiveness and practical value:

RQ1: Can ATFS effectively break "defense silos" and achieve universal defense across heterogeneous generative models, outperforming specialized methods and existing ensemble strategies?

RQ2: Is the feature-space alignment mechanism underlying ATFS truly architecture-independent, capable of protecting a broader range of generative models (e.g., VQ-VAE)?

RQ3: What are the computational efficiency, convergence speed, and perturbation imperceptibility of ATFS—key metrics for real-world deployment?

RQ4: Can adversarial examples generated by ATFS withstand common signal distortions encountered during image transmission and processing (e.g., compression, scaling)?

RQ5: Does the defense effectiveness of ATFS remain consistent across different demographic attributes (e.g., gender, race), avoiding algorithmic bias?

4.1 Experimental Setup

To comprehensively assess the defense methods within a Trustworthy and Responsible AI framework[21], we adopt a multi-dimensional evaluation setup encompassing the following aspects:

Datasets and Models: Experiments were conducted on a subset of the widely used VGG-Face2 dataset[22]. To simulate heterogeneous threat environments, we constructed two core scenarios:

Scenario A (DM + GAN): Combines Stable Diffusion v1.5 (based on probability density modeling) and StarGAN v2[11] (based on discriminant boundaries).

Scenario B (DM + VAE): Includes Stable Diffusion v1.5 and VQ-VAE (based on discrete codebook reconstruction).

Baseline Methods: We selected four categories of representative baselines: (1) SOTA Architecture-Specific Methods: *Mist*[9] for diffusion models, *Anti-Forgery*[10] for GANs, and standard PGD attack for VQ-VAE; (2) Naive Joint Method: Aggregating the loss gradients for different models via simple summation in pixel space; (3) Gradient Correction Method: Applying the *PCGrad*[15] algorithm with gradient coordination (denoted as PCGrad Coordinated) to project and rectify conflicting gradients from heterogeneous models.

Evaluation Metrics: For image generation and model fine-tuning tasks (e.g., DreamBooth[23]), the core objective is to prevent the model from learning a specific visual concept (e.g., a person’s face). We use FID[24] to quantify the distance between generated images and the real distribution, and IL-NIQE[25] to assess perceptual quality. Higher values indicate greater deviation from the original concept and lower quality, signifying successful protection. For image editing and translation tasks (e.g., SDEdit, StarGANEdit[11], VAE Reconstruction), the focus is on disrupting editing accuracy. We use MS-SSIM and PSNR[25] to measure similarity between the attacked result and the ideal (unattacked) edit, alongside IL-NIQE. Here, lower MS-SSIM/PSNR and higher IL-NIQE indicate severe distortion of the editing result, proving effective defense.

Implementation Details: All experiments were performed on an NVIDIA RTX 3090 GPU. Default settings for ATFS: iterations $T = 100$, perturbation budget $\epsilon = 6/255$, step size $\alpha = \epsilon/10$, with a structured noise image serving as the feature anchor.

4.2 Core Effectiveness (RQ1)

This experiment verifies the core defense capability of ATFS in the heterogeneous DM + GAN scenario. We design the evaluation in two aspects: 1) verifying the direct effectiveness of adversarially trained examples on their target editing tasks (SDEdit for DM and StarGANEdit for GAN); 2) validating the transferability of these examples to another diffusion-based model, DreamBooth, without any retraining.

4.2.1 Defense Performance on SDEdit and StarGANEdit. As shown in Table 1, existing methods generally exhibit a “defense silo” effect. MIST is effective against SDEdit (MS-SSIM: 0.6387) but its performance drops sharply against StarGANEdit (MS-SSIM: 0.8011); Anti-Forgery shows the opposite trend. This demonstrates the limitation of architecture-specific optimization. Although the naive joint attack and the PCGrad correction method achieve some cross model effects, their performance is significantly lower than that of ATFS. For instance, in the StarGANEdit task, the MS-SSIM of ATFS (0.5228) is much lower than that of PCGrad (0.6204). ATFS attains the best values across all metrics on both editing tasks, proving its ability to enable effective universal defense through feature-level synergy.

Notably, ATFS not only excels in cross-model defense but even surpasses state-of-the-art specialized methods on their respective single-model defense tasks. This phenomenon stems from a fundamental shift in the adversarial paradigm: although Mist operates in the VAE latent space (a feature space) of diffusion models, its attack target is essentially the model-specific denoising trajectory or encoder feature distance. In contrast, ATFS interferes with the cross-model shared high-level feature alignment space via the target guidance image, achieving more thorough feature-level distortion.

Table 1: Quantitative Results on DM+GAN Heterogeneous Defense

Method	SDEdit			StarGANEdit		
	MS-SSIM↓	PSNR↓	IL-NIQE↑	MS-SSIM↓	PSNR↓	IL-NIQE↑
Original	0.8516	31.26	28.1654	0.9989	49.94	30.3326
MIST	0.6387	20.65	39.6495	0.8011	24.43	32.1648
Antiforgery	0.7534	26.42	33.7946	0.5464	15.29	42.4615
Naive joint	0.6812	21.22	35.3013	0.6503	17.78	38.7418
PCGrad Coordinated	0.6563	20.85	37.6615	0.6204	16.46	39.3195
Ours	0.5122	18.69	41.2712	0.5228	13.63	43.3251

Similarly, while Anti-Forgery attacks the GAN’s output layer by adding perturbations in pixel space—a model-specific adversarial game—ATFS directly disrupts the generator’s encoding core at the feature-space level. This empirically validates that attacking the cross-model shared high-level feature alignment space (a higher-level, architecture-agnostic representation layer) is inherently more disruptive than targeting low-level mechanisms specific to individual models.

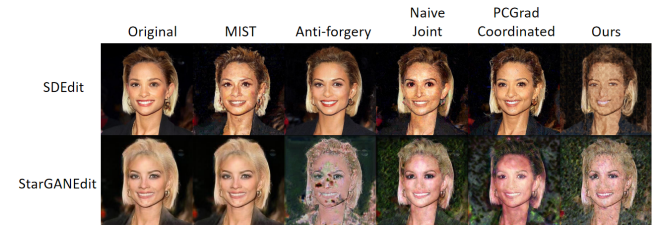


Figure 3: Qualitative Visualization of Cross-Architecture Defense Effects

As illustrated in Figure 3, the visual results align with the quantitative analysis. Images protected by MIST fail to be edited by SDEdit, yet StarGANEdit can still successfully alter hair color; images protected by Anti-Forgery show the opposite trend. In contrast, images protected by ATFS produce completely distorted outputs from both editors, with no facial identity features preserved. This visually verifies that ATFS, through its feature synergy mechanism, achieves reliable dual protection against heterogeneous models with a single perturbation, fundamentally breaking the “defense silo.”

4.2.2 Transferability to Unseen Diffusion-based Model (DreamBooth). To further validate the generalization capability of our method across models within the same generative paradigm, we directly apply the adversarial examples trained for the DM+GAN scenario to DreamBooth, which is another diffusion-based model designed for subject-driven generation, without any retraining or adaptation. As shown in Figure 4, the adversarial examples generated by ATFS effectively disrupt DreamBooth’s ability to learn and reconstruct the target identity. The model fails to generate coherent images of the protected subject, producing instead distorted or irrelevant content.

This transferability demonstrates that the perturbations generated by ATFS are not only effective against the specific diffusion



Figure 4: Transferability to DreamBooth. Adversarial examples generated by ATFS effectively disrupt subject-driven generation in DreamBooth

model (SDEdit) used during training but also generalize successfully to another diffusion-based architecture (DreamBooth). This capability stems from ATFS’s core mechanism: by attacking the shared high-level feature space rather than model-specific low-level mechanisms, it creates perturbations that maintain effectiveness across models within the same paradigm.

4.3 Generalizability Verification (RQ2)

To verify whether our framework is constrained to specific model combinations, we evaluate ATFS in the ‘DM + VQ-VAE’ scenario. VQ-VAE relies on discrete codebook reconstruction, a mechanism fundamentally different from both DMs and GANs. We execute the attack by solely switching the corresponding model’s feature extractor (encoder), without altering the underlying algorithmic logic.

4.3.1 Direct Defense Performance on SDEdit and VAE Reconstruction. As shown in Table 2, specialized methods like MIST are nearly ineffective against VQ-VAE (MS-SSIM: 0.9194), confirming the architectural limitations of existing approaches. In contrast, ATFS achieves significantly better performance on VAE reconstruction (MS-SSIM: 0.7443) while maintaining strong results on SDEdit, demonstrating its architecture-agnostic capability. Qualitative results are presented in Figure 5.

Table 2: Quantitative Results on DM+VQ-VAE Architecture Generalization

Method	SDEdit			VAE Reconstruction		
	MS-SSIM↓	PSNR↓	IL-NIQE↑	MS-SSIM↓	PSNR↓	IL-NIQE↑
MIST	0.6177	17.86	40.5124	0.9194	29.74	31.3451
PGD	0.6828	23.17	35.2631	0.7668	19.41	35.2115
Naive joint	0.6614	22.03	35.5144	0.7961	20.31	34.2142
PCGrad	0.6536	20.67	37.1154	0.8183	21.85	33.8145
Coordinated	0.6536	20.67	37.1154	0.8183	21.85	33.8145
Ours	0.5215	18.78	41.0214	0.7443	16.51	36.7187

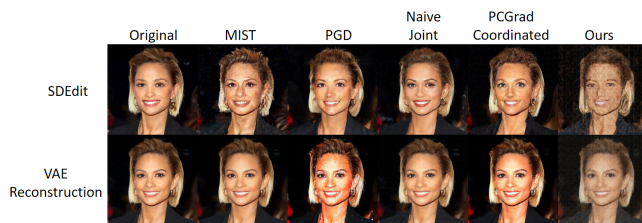


Figure 5: Qualitative Results on DM + VQ-VAE Scenario

4.3.2 Scalability to Multiple Heterogeneous Models. To rigorously evaluate ATFS’s extensibility, we test defense against three heterogeneous models simultaneously: a diffusion model (Stable Diffusion), a GAN (StarGAN), and a VQ-VAE. This challenging scenario evaluates the framework’s capacity to handle increased architectural diversity within a unified optimization.

Figure 6 shows qualitative results where a single ATFS-generated perturbation concurrently disrupts all three generation processes. The adversarial examples cause: (1) identity loss in SDEdit outputs, (2) structural distortion in StarGANedit results, and (3) perceptual corruption in VQ-VAE reconstructions. This demonstrates that feature-space alignment scales effectively to multi-model defense.



Figure 6: Cross-Architecture Defense Effectiveness. Each row represents a test example.

Importantly, ATFS achieves this without algorithmic modifications. Defending an additional model requires only incorporating its feature extractor Φ_k and target feature t_k into the existing optimization objective (Eq. 7). This plug-and-play extensibility—avoiding attack redesign or hyperparameter tuning—highlights the practicality of our feature-space approach for real-world environments containing diverse generative architectures.

4.4 Practicality Analysis (RQ3)

We systematically evaluate the defense effectiveness of ATFS under varying perturbation budgets $\epsilon \in 2/255, 4/255, 8/255, 16/255$ (Table 3). The results demonstrate that ATFS maintains strong efficacy even under a strict imperceptibility budget $\epsilon = 2/255$, significantly disrupting both SDEdit (MS-SSIM: 0.646) and StarGANedit (MS-SSIM: 0.5915). Notably, the performance gain exhibits diminishing marginal returns as ϵ increases, indicating that most of the defensive effect is achieved with minimal pixel-level distortion. This efficiency aligns with our theoretical insight: by operating in a shared feature space, ATFS induces maximal feature-level distortion per unit of pixel change. Consequently, ATFS offers a favorable trade-off between attack potency and visual stealth, making it suitable for real-world deployment where perturbation visibility is critical.

Table 3: Performance Comparison under Different Perturbation Budgets

Perturbation budget	SDEdit			StarGANedit		
	MS-SSIM↓	PSNR↓	IL-NIQE↑	MS-SSIM↓	PSNR↓	IL-NIQE↑
2/255	0.646	20.56	38.6471	0.5915	15.61	39.4461
4/255	0.5834	19.67	39.5461	0.554	15.9	40.3215
8/255	0.4807	18.26	40.8471	0.426	15.09	42.5147
16/255	0.4047	17.08	42.7214	0.2914	13.24	46.1541

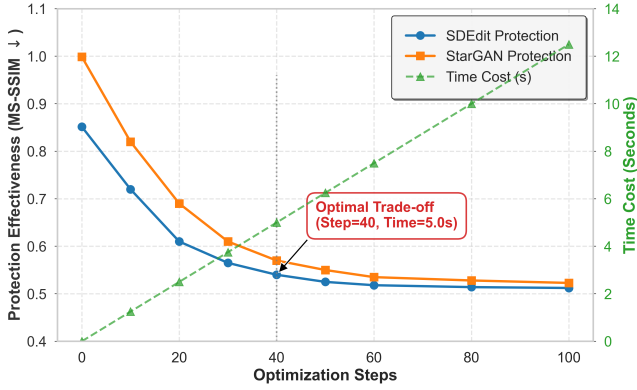


Figure 7: Efficiency Analysis: Protection Effectiveness vs. Time Cost

Convergence and Trade-off: To intuitively quantify the trade-off between performance and overhead, Figure 7 employs a dual-axis visualization. The solid curves (Protection Effectiveness) show a steep descent in the initial phase, while the dashed line (Time Cost) grows linearly. We identify an "Optimal Trade-off" point: ATFS requires only 40 iterations (approx. 5.0s) to achieve over 90% of its final converged performance. This efficiency benefits from the target guidance image providing a clear global optimization direction, drastically reducing oscillation in heterogeneous gradient fields. Unlike PCGrad, which requires costly projections, ATFS’s linear aggregation makes it highly suitable for real-time privacy protection systems.

4.5 Robustness Analysis (RQ4)

In real-world social media transmission, images inevitably undergo lossy compression or noise interference. We simulated three common signal distortions: Gaussian noise, JPEG compression, and Scaling.

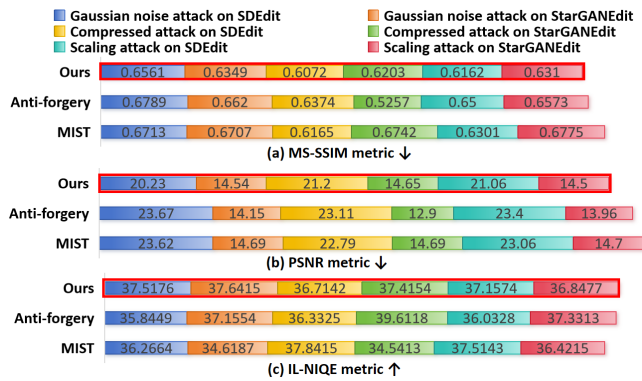


Figure 8: Robustness Analysis: Performance under Various Attack Scenarios

As shown in Figure 8, while all methods suffer some degradation, ATFS maintains the strongest protection across all scenarios. Particularly in the challenging JPEG compression scenario, baseline

methods like Anti-Forgery see significant efficacy drops (MS-SSIM rises to 0.6374). This is because traditional pixel-level attacks often rely on minute high-frequency noise patterns, which are easily filtered out during JPEG’s Discrete Cosine Transform (DCT) and quantization. In contrast, ATFS maintains a low MS-SSIM of 0.6072. This advantage stems from our fundamental shift from attacking shallow pixel space to the high-level feature space. Since feature representations inherently possess scale invariance and noise resistance, adversarial perturbations generated via feature synergy successfully inherit these robust properties.

4.6 Fairness Analysis (RQ5)

To ensure ATFS does not introduce algorithmic bias, we evaluated its performance across facial images with different attributes (Gender, Age, Race).

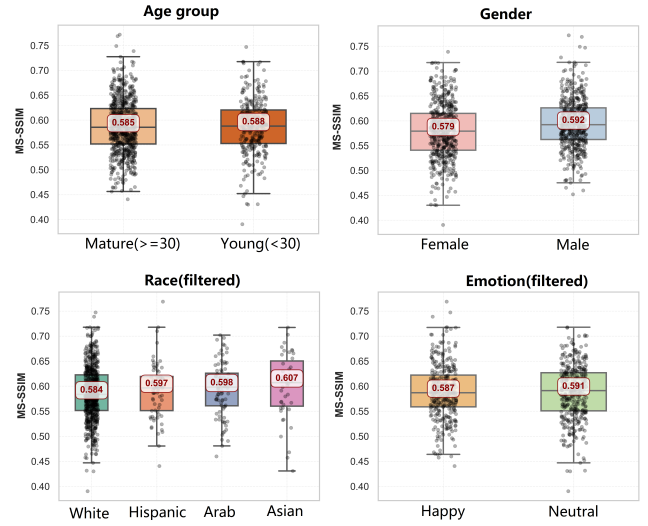


Figure 9: Performance Variation Analysis across Different Demographic Groups

As illustrated in Figure 7, the box plots of defense performance (MS-SSIM) for different subgroups (e.g., Male vs. Female, different racial groups) highly overlap, with very close medians. The Kruskal-Wallis test further confirms no statistically significant difference in performance distribution among attribute groups ($p > 0.05$). This proves that ATFS delivers fair and consistent protection, avoiding uneven defense based on demographic attributes, which aligns with the ethical requirements of Responsible AI.

5 Conclusion

Confronted with the threat of heterogeneous generative models in the wild, existing proactive defense methods are trapped in "Defense Silos" due to their architecture-specificity. This paper identifies the root cause as the fundamental conflict of optimization objectives among heterogeneous models in pixel space, which hinders gradient synergy. To address this, we propose a novel defense paradigm based on the empirical observation of feature space alignment across different architectures. We design the Architecture-Agnostic

Targeted Feature Synergy (ATFS) framework. By utilizing a target guidance image to unify heterogeneous defenses into a feature space alignment task, ATFS achieves gradient alignment theoretically and enables efficient, lightweight perturbation generation practically (e.g., ~ 2 seconds per image, compared to > 15 s for gradient projection baselines). Experiments demonstrate that ATFS achieves SOTA performance in heterogeneous scenarios and easily extends to other architectures. The method is effective under low perturbation budgets, robust against common signal distortions, and fair across diverse demographics, offering a practical solution for Trustworthy Generative AI safety that balances efficiency and reliability. Future work will focus on three directions: 1) dynamic target feature direction search for maximal disruption; 2) extension to 3D spatiotemporal feature spaces for video protection.

References

- [1] R. Rombach, A. Blattmann, D. Lorenz, P. Esser, and B. Ommer, "High-resolution image synthesis with latent diffusion models," in *Proceedings of the IEEE/CVF Conference on Computer Vision and Pattern Recognition*, pp. 10684–10695, 2022.
- [2] I. Goodfellow, J. Pouget-Abadie, M. Mirza, B. Xu, D. Warde-Farley, S. Ozair, A. Courville, and Y. Bengio, "Generative adversarial nets," in *Advances in Neural Information Processing Systems*, pp. 2672–2680, 2014.
- [3] L. Zheng, N. Yu, A. Saberi, M. Backes, M. Fritz, and Y. Zhang, "Unganable: Defending against gan-based face manipulation," in *32nd USENIX Security Symposium (USENIX Security 23)*, pp. 7213–7230, 2023.
- [4] I. Korshunova, W. Shi, J. Dambre, and L. Theis, "Fast face-swap using convolutional neural networks," in *Proceedings of the IEEE International Conference on Computer Vision*, pp. 3697–3705, 2017.
- [5] J. Smith and B. Johnson, "The graph structure of diffusion networks in on-line misinformation campaigns," in *Proceedings of The Web Conference (WWW)*, pp. 200–212, 2024.
- [6] J. C. Costa, T. Roxo, H. Proença, and P. R. M. Inacio, "How deep learning sees the world: a survey on adversarial attacks & defenses," *IEEE Access*, vol. 12, pp. 61113–61136, 2024.
- [7] J. Liu, Y. Li, Y. Guo, Y. Liu, J. Tao, and Y. Niu, "Generation and countermeasures of adversarial examples on vision: A survey," *Artificial Intelligence Review*, vol. 57, no. 8, p. 199, 2024.
- [8] H. Chen, Q. Xiang, J. Hu, M. Ye, C. Yu, H. Cheng, and L. Zhang, "Comprehensive exploration of diffusion models in image generation: a survey," *Artificial Intelligence Review*, vol. 58, no. 4, p. 99, 2025.
- [9] C. Liang and X. Wu, "Mist: Towards improved adversarial examples for diffusion models," *arXiv preprint arXiv:2305.12683*, 2023.
- [10] R. Wang, Z. Huang, Z. Chen, L. Li, J. Chen, and L. Wang, "Anti-forgery: Towards a stealthy and robust deepfake disruption attack via adversarial perceptual-aware perturbations," *arXiv preprint arXiv:2206.00477*, 2022.
- [11] Y. Choi, M. Choi, M. Kim, J.-W. Ha, S. Kim, and J. Choo, "Stargan: Unified generative adversarial networks for multi-domain image-to-image translation," in *Proceedings of the IEEE Conference on Computer Vision and Pattern Recognition*, pp. 8789–8797, 2018.
- [12] W. Zhang and H. Li, "A comprehensive threat model for generative ai-powered cyber attacks," in *Proceedings of the ACM SIGSAC Conference on Computer and Communications Security*, pp. 55–70, 2023.
- [13] Y. Song, J. Sohl-Dickstein, D. P. Kingma, A. Kumar, S. Ermon, and B. Poole, "Score-based generative modeling through stochastic differential equations," *International Conference on Learning Representations (ICLR)*, 2021.
- [14] R. Vershynin, *High-Dimensional Probability: An Introduction with Applications in Data Science*, vol. 47. Cambridge University Press, 2018.
- [15] T. Yu, S. Kumar, A. Gupta, S. Levine, K. Hausman, and C. Finn, "Gradient surgery for multi-task learning," in *Advances in Neural Information Processing Systems*, vol. 33, pp. 5824–5836, 2020.
- [16] O. Sener and V. Koltun, "Multi-task learning as multi-objective optimization," in *Advances in Neural Information Processing Systems*, vol. 31, 2018.
- [17] S. Lin, X. Zhang, W. Susilo, X. Chen, and J. K. Liu, "Gdr-gma: Machine unlearning via directionrectified and magnitude-adjusted gradients," in *Proceedings of the 32nd ACM International Conference on Multimedia*, pp. 9087–9095, 2024.
- [18] S. Shin, J. Chen, E. Wexler, H. Zhang, R. Han, and B. Y. Zou, "Glaze: Protecting artists from style mimicry by text-to-image models," *arXiv preprint arXiv:2302.04222*, 2023.
- [19] B. Zhang, Y. Song, F. Zhang, and W.-C. Lee, "Design and implementation of decentralized data protection protocol for generative ai," in *Proceedings of the 30th International Conference on Database Systems for Advanced Applications*, 2025.
- [20] C. Zhao, B. Vijay, C.-Y. Lee, and A. Rabinovich, "Gradnorm: Gradient normalization for adaptive loss balancing in deep multitask networks," in *International Conference on Machine Learning*, pp. 794–803, PMLR, 2018.
- [21] T. Lin, M. Yen, C. Meng, Y. Mao, R. Jia, A. Raghunathan, and L. Schmidt, "Holistic evaluation of text-to-image models," in *Advances in Neural Information Processing Systems*, vol. 36, pp. 49181–49201, 2023.
- [22] Q. Cao, L. Shen, W. Xie, O. M. Parkhi, and A. Zisserman, "Vggface2: A dataset for recognising faces across pose and age," in *2018 13th IEEE International Conference on Automatic Face & Gesture Recognition (FG 2018)*, pp. 67–74, IEEE, 2018.
- [23] N. Ruiz, Y. Li, V. Jampani, Y. Pritch, M. Rubinstein, and K. Aberman, "Dreambooth: Fine tuning text-to-image diffusion models for subject-driven generation," in *Proceedings of the IEEE/CVF Conference on Computer Vision and Pattern Recognition*, pp. 22500–22510, 2023.
- [24] M. Heusel, H. Ramsauer, T. Unterthiner, B. Nessler, and S. Hochreiter, "Gans trained by a two time-scale update rule converge to a local nash equilibrium," *Advances in Neural Information Processing Systems (NeurIPS)*, vol. 30, 2017.
- [25] C. Ma, Z. Sun, Z. Lv, S. Xu, F. Chen, and Y. Sun, "A survey on image quality assessment: Insights, analysis, and future outlook," *arXiv preprint arXiv:2502.08540*, 2025.

A Visual Effects under Different Perturbation Budgets

This appendix provides an extended visual analysis of adversarial examples and their defensive effects under different perturbation budgets (ϵ), supplementing Section 4.4 of the main text.

Figure A.1 systematically illustrates the impact of the perturbation budget $\epsilon \in \{2/255, 4/255, 8/255, 16/255\}$ on defense effectiveness. Each column corresponds to a specific ϵ value.

The visual results are highly consistent with the quantitative data in Table 4 of the main text. As ϵ increases, the output quality of both SDEdit and StarGANedit deteriorates sharply. At $\epsilon = 16/255$, the outputs from both editors completely lose the original identity information, becoming unrecognizable abstract patterns or noise, successfully achieving content protection.

Even at $\epsilon = 2/255$, while the visual quality of the adversarial example remains high, it already causes noticeable disruption to the editing results. This provides flexibility for practical applications: a smaller budget can be chosen for scenarios with stringent imperceptibility requirements, while a larger budget can be used for higher security demands.



Figure A.1: Visualization of ATFS Defense under Varying Perturbation Budgets